arXiv:cond-mat/0312604v2 [cond-mat.mes-hall] 10 Jan 2004

Dynamics of twin-condensate configurations in an open chain of three Bose-Einstein condensates

P. Buonsante[1], R. Franzosi[2], and V. Penna[1]

[1]*Dipartimento di Fisica & Unità INFM, Politecnico di Torino,*
Corso Duca degli Abruzzi 24, I-10129 Torino, Italy
[2]*Dipartimento di Fisica & Sezione INFN, Università di Pisa,*
Via Buonarroti 2, I-56127 Pisa, Italy.

February 2, 2008

Abstract – The dynamics of a mean-field model of three coupled condensates is studied for initial states characterized by twin condensates. Condensates occupy an open three-well chain, where the central potential-well depth is an independent parameter. Despite its diversity from the closed-chain symmetric model, such model is shown to have an integrable regime involving a predictable evolution for twin-condensate initial states. After establishing the dependence of the phase-space topology on the model parameters, the latter are shown to allow the control of various macroscopic effects such as rapid population inversions, pulsed phase changes, self-trapping and long-duration periodic oscillations. Finally, based on quantizing the system in terms of suitable "microscopic" canonical variables, the stability conditions of the integrable regime are related to the su(1,1) structure of the Hamiltonian spectrum.

Conference topic: Bose-Eistein condensation of trapped atoms. **Program report number**: 6.3.1

PACS: 74.50.+r, 03.65.Fd, 05.30.Jp, 03.75.Fi

e-mail address: penna@polito.it

1. INTRODUCTION

The increasing skill in realizing experimental set-up's where Bose-Einstein condensates (BEC) are distributed in potential wells with complex space structures [1, 2] has prompted, over the last few years, the study of models such as the two-well system (dimer) [3, 4, 5, 6], the three-well system (TWS) [7, 8, 9], and their many-well generalization such as the linear chain [10] of coupled BECs. An aspect that has raised particular interest is the recognition of characteristic behaviors and macroscopic phenomena that distinguish the dynamics of coupled wells. The latter consists of interwell boson exchanges enacted by the tunnel effect [11] that determine, in each well, macroscopic changes of the condensate phase and population.

The study of the TWS on a closed chain (three wells mutually coupled) has revealed, within a dynamics dominated by chaos [12], the presence of an integrable subregime [8, 9] corresponding to (a phase-space submanifold of) states in which two of the three wells exhibit identical condensate phases and boson numbers per well. Such twin-condensate (TC) configurations are preserved dynamically and make the TWS equivalent, in practice, to a two-well system. Particularly, the dimer integrability [6] is inherited by

TWS when this is prepared in an initial state with TCs.

The TWS integrable subdynamics raises interest for various reasons. First, achieving a full knowledge of the TWS phenomenology with a regular dynamical character (this extends the analysis of Ref. [13]) is necessary to design significant experiments. Second, since perturbing dimerlike states leads to prime chaotic behaviors, the modalities governing their onset (namely the preparation of suitable initial states priming chaos) are a central aspect. This is important, not only for the TWS, but also for the new class of systems (coupled-BEC chains) whose control, at the experimental level, is rapidly increasing. Finally, in view of the last observation, the recognition of a class of states having regular time behaviors (near those showing chaos) is certainly useful to study the manifestation of classical instabilities at the quantum level.

In this paper we consider the open TWS, namely a three-well system in which two decoupled (lateral) wells interact with a third (central) one. In particular, we show that, as in the closed-chain case, the open-TWS dynamics is equipped with an integrable subregime. To do this, we find new coordinates that both account for the dynamical constraint embodying the TC form and preserve the canonical structure in the TC subdynamics without resorting to Dirac's procedure for constrained Hamiltonians. As to the possibility to influence the system dynamical behaviour (and thus to play a relevant role in designing possible controlled experiments), we point out that in addition to the tunneling parameter (denoted by T) the open TWS model exhibits a further adjustable parameter w that distinguishes the central potential-well depth from the two (equal) lateral-well depths.

The present analysis prosecutes the work both of Ref. [9] concerning the self-trapping onset in the dimerlike regime of the symmetric ($w = 0$) closed TWS, and of Ref. [13]. In the latter the analysis of the fixed points and the origin of chaotic behaviors in the open TWS were embodied, for arbitrary T and w, in two dynamical phase diagrams (relevant to the dimerlike and nondimerlike classes of fixed points) that supply an exhaustive, operationally valuable, account of the system stability.

In the sequel, we concentrate on the dynamics of TC configurations and, more specifically, on the features "in large" of orbit bundles that characterize the topology of the reduced phase space in the dimerlike sub-regime. We investigate both the conditions under which the system evolution exhibits either oscillatory or ballistic motion, and the possibility to control the self-trapping and other effects through the parameters T and w. Also, we show that the independence of parameter w, which introduces further asymmetry in the model-Hamiltonian structure but improves the possibility of fitting experimental conditions, does not affect the (partial) integrability of TWS and enriches noticeably the dynamical scenario of the system. Finally, we evaluate the stability of TC dynamics under quantum perturbations by partially recovering the quantized form of the TWS Hamiltonian. To this end the dynamical degrees of freedom that, within the new canonical coordinates mentioned above, account for the deviation from dimeric regime, naturally undergo the quantization when they have a nonmacroscopic character. The stability of dimerlike configurations will be proven by relying on the su(1,1) structure exhibited by the model Hamiltonian.

2. TRIMER-DYNAMICS CANONICAL FORM

The asymmetric TWS we consider here is described by the second-quantized Hamiltonian

$$H = U \sum_{i=1}^{3} n_i^2 - v(n_1 + n_3) - v_2 n_2$$

$$- \frac{T}{2} \left(a_1^\dagger a_2 + a_1^\dagger a_3 + h.c. \right) , \qquad (1)$$

which one derives from the many-body quantum theory of BECs through a three-mode expansion of the condensate field operator [8]. Parameters U, T, v, account for the interatomic scattering, the tunneling amplitude, and the sided-well potential depth, respectively; the central-well depth has, in general, an independent value $v_2 = v + w \neq v$. Another element of diversity from the symmetric-TWS case is due to the absence of interwell coupling between the first and the third well. The operators $n_i \doteq a_i^\dagger a_i$ count the bosons in the ith well ($N = \Sigma_i n_i$), while the destruction(creation) operators a_i ($a_i^\dagger$) obey the canonical commutators $[a_i, a_\ell^\dagger] = \delta_{i\ell}$. Preceding studies of the TWS dynamics have been focused on a case where the asymmetric character issues from nonconstant tunneling parameters T_{ij} such that $T_{12} \gg T_{13} = T_{23} = T$. Classically ($a_\ell^\dagger \equiv a_\ell^*$, $a_i a_\ell^\dagger = a_\ell^\dagger a_i$), the asymmetric TWS has revealed [7] the presence of homoclinic chaos, while, quantally, the survival of breather configurations has been investigated on the trimer viewed as the smallest possible closed chain. The Heisenberg equations related to H for the boson operators a_i, $a_i^\dagger$ give, within the random-phase approximation, the equations ($s = 1, 3$)

$$\begin{aligned} i\hbar\dot{z}_s &= (2U|z_s|^2 - v)z_s - \tfrac{T}{2} z_2 \, , \\ i\hbar\dot{z}_2 &= [2U|z_2|^2 - (w+v)]z_2 - \tfrac{T}{2}(z_3 + z_1) \, , \end{aligned} \tag{2}$$

for the expectation values $z_i = \langle a_i \rangle$, $z_i^* = \langle a_i^\dagger \rangle$, of the three wells. These entail $\Sigma_i |z_i|^2$ as a conserved quantity replacing the (conserved) total boson number N ($[N, H] = 0$). Eqs. (2) can be also obtained from

$$\mathcal{H}(Z, Z^*) \equiv U \sum_{j=1}^{3} |z_j|^4 - v(|z_1|^2 + |z_3|^2)$$
$$-(v+w)|z_2|^2 - \frac{T}{2}(z_2^* z_3 + z_2^* z_1 + c.c.)$$

by using the standard canonical Poisson brackets $\{z_k^*, z_j\} = i\delta_{kj}/\hbar$. The latter and $\mathcal{H}(Z, Z^*)$ can be also derived variationally within the coherent-state approach developed in Refs. [14, 21].

Sub-dynamics of Twin-Condensate configurations. Based on Eqs. (2), imposing the constraint $z_1 = z_3$ leads to identify an integrable subregime of TWS dynamics which consists of the orbit bundles lying on the sub-manifold $\mathcal{P} := \{(z_1, z_2, z_3) : z_1 = z_3, z_2 \in \mathbf{C}\}$ in the original phase space $\mathcal{M}$. This can be proven by introducing the new canonical variables $\xi = (z_1 - z_3)/\sqrt{2}$, $z = (z_1 + z_3)/\sqrt{2}$ such that $\{\xi^*, \xi\} = i/\hbar = \{z^*, z\}$, and $\{z^*, \xi\} = \{\xi^*, z_2\} = \{z_2^*, z\} = 0$. One finds that

$$H = \frac{U}{2}\left[(|z|^2 + |\xi|^2)^2 + (z\xi^* + z^*\xi)^2 + 2|z_2|^4\right]$$
$$- v\mathcal{N} - w|z_2|^2 - \frac{T}{\sqrt{2}}(z_2 z^* + z_2^* z) \tag{3}$$

($\mathcal{N} = \Sigma_i |z_i|^2 = |z_2|^2 + |z|^2 + |\xi|^2$) giving, in turn,

$$i\hbar\dot{z} = U(|z|^2 + |\xi|^2)z - vz + U(z\xi^* + z^*\xi)\xi - \frac{T}{\sqrt{2}} z_2 \, ,$$
$$i\hbar\dot{z}_2 = [2U|z_2|^2 - (v+w)]z_2 - \frac{T}{\sqrt{2}} z \, , \tag{4}$$
$$i\hbar\dot{\xi} = U(|z|^2 + |\xi|^2)\xi - v\xi + U(z\xi^* + z^*\xi)z \, .$$

Setting $\xi = 0$ (that is $z_1 = z_3$) eliminates the third equation, while the remaining pair of coupled equations, with the substitution $z = \sqrt{2} z_1$,

$$\left\{ \begin{aligned} i\hbar\dot{z}_1 &= (2U|z_1|^2 - v)z_1 - \tfrac{T}{2} z_2 \\ i\hbar\dot{z}_2 &= [2U|z_2|^2 - (v+w)]z_2 - T z_1 \, , \end{aligned} \right. \tag{5}$$

coincide with Eqs. (2) under the restriction $z_1 = z_3$ to the sub-manifold $\mathcal{P}$. The two costants of motion corresponding to the energy

$$H_0 = U\left(\frac{1}{2}|z|^4 + |z_2|^4\right) - v|z|^2$$
$$-(v+w)|z_2|^2 - \frac{T}{\sqrt{2}}(z_2 z^* + z_2^* z)$$

and the total boson number $N = 2n_1 + n_2 = |z|^2 + |z_2|^2$ ($n_i \equiv |z_i|^2$) make the dynamics issuing from Eqs. (5) integrable. Notice that, while H_0 still generates the correct equations for z and z_2 through $\dot{z} = \{z, H_0\}$, $\dot{z}_2 = \{z_2, H_0\}$, the same Hamiltonian written in terms of z_1, z_2 no longer provides Eqs. (5). The useful role of the variables z, z_2, ξ is thus to supply a new canonical scheme where the restriction to $\mathcal{P}$ can be enacted directly on H bypassing Dirac's scheme for constrained systems. The resulting Hamiltonian H_0 can be further cast in the pendulum-like version

$$H_0 = C_0 + \frac{3U}{8}D^2 - \frac{f_\nu}{4}D - \frac{T}{\sqrt{2}}\sqrt{N^2 - D^2}\cos 2\theta\,,$$

in which the motion constant N is used explicitly, $C_0 = 3UN^2/8 - N(v + w/2)$, $f_\nu = UN(1 - 2\nu)$, $\nu = w/UN$, and $\theta := (\phi_2 - \phi)/2$ [defined through $z = |z|\exp(i\phi)$, $z_2 = |z_2|\exp(i\phi_2)$] and $D := |z|^2 - |z_2|^2$ fulfill the brackets $\{\theta, D\} = 1/\hbar$. The ensuing representation on the plane (θ, D) is the simplest possible way to describe the space $\mathcal{P}$ and its structure changes when T, U, w are varied. Such a $\theta - D$ picture involves two equations

$$\hbar\dot{\theta} = \frac{3}{4}UD - \frac{f_\nu}{4} + \frac{TD\cos 2\theta}{\sqrt{2}\sqrt{N^2 - D^2}}\,, \tag{6}$$

$$\hbar\dot{D} = -\sqrt{2}T\sqrt{N^2 - D^2}\,\sin 2\theta\,, \tag{7}$$

only. The other pair of canonical variables $\psi = (\phi_2 + \phi)/2$, $N = |z|^2 + |z_2|^2$, in fact, do not participate in the dynamics: while $\dot{N} = 0$, the angle ψ plays an auxiliary role since $\dot{\psi}$ can be proven to be completely determined by the evolution of θ and D which, on the contrary, have ψ-independent equations.

3. PHASE-SPACE STRUCTURE AND PARAMETER DEPENDENCE

The TWS integrable subdynamics is reducible to a one-dimensional potential problem with an unique (phase-independent) EN-dependent equation $\dot{D}^2 = f(D; E, N)$ for D by implementing standard quadrature procedures [9, 16]. The latter lead to solve explicitly the motion equations in terms of elliptic functions. Nevertheless, the analytic complexity of the one-dimensional potential makes rather difficult to establish the dependence on τ and ν of the $\mathcal{P}$ structure as well as of the dynamics therein represented. Then, since we wish to recognize the features that distinguish the dynamical behaviors of TC configurations [rather than the exact analytic solutions of Eqs. (6), (7)], we simply approach the problem by performing in parallel the study of the fixed points of Eqs. (6), (7) and the numerical reconstruction of the phase-space portraits. This furnishes in a quite direct way information on both the topology changes in $\mathcal{P}$ when τ and ν are varied, and the features "in large" of the dimerlike bundles of trajectories represented on the $\theta - D$ plane. In particular, the conditions that cause variuos macroscopic effects in the dynamical behavior can be evidenced effectively.

The equation pair that determine the fixed points, $0 = [3UD - f_\nu + 2\sqrt{2}TD\cos(2\theta)/r(D)]/4$, $0 = \sqrt{2}Tr(D)\sin(2\theta)$ with $r(D) = \sqrt{N^2 - D^2}$, is stemmed from equations (6), (7) when setting $\dot{\theta} = 0 = \dot{D}$.

These supply maxima, saddles and minima that constitute the fixed-points set in the reduced phase space $\mathcal{P}$. The minimum is situated in $\theta = 0$, $D \neq 0$ ($D = 0$ only for $\nu = 1/2$), while the other extremal points stay on the straight line $\theta = \pi/2$. Under such conditions, the values of D at fixed-points are obtained from the nonlinear equation

$$0 = \frac{3}{4}X - \frac{1 - 2\nu}{4} + \frac{\sigma\tau X}{\sqrt{2}\sqrt{1 - X^2}} \tag{8}$$

where $\sigma = +1$ ($\sigma = -1$) in the case of the minimum (maxima/saddles), and the adimensional quantities $\tau := T/UN$, $X = D/N$ have been introduced in addition to $\nu := w/UN$. The number of fixed point as a function of ν, τ is easily deduced from eq. (8). In the parameter space (ν, τ), the critical lines

$$\nu_r = \frac{1}{2} + (-)^r\,\frac{3}{2}\left[1 - 2\left(\frac{\tau}{3}\right)^{2/3}\right]^{3/2}\,,$$

($r = 1, 2$) are recognized to play a crucial role. For $\nu_1(\tau) < \nu < \nu_2(\tau)$ ($\nu = \nu_1(\tau), \nu_2(\tau)$) three (two) solutions are furnished by equation (8) with $\sigma = -1$, in addition to the permanent single solution of the case $\sigma = +1$. The lobe

$$\mathcal{L} = \{(\nu, \tau) : 0 < \tau < 3/\sqrt{8},\ \nu_1(\tau) < \nu < \nu_2(\tau)\},$$

defined in the parameter plane (ν, τ) identifies completely the area corresponding to the three-solution regime. Outside $\mathcal{L}$, only one solution survives together with the solution of the case $\sigma = +1$.

4. TOPOLOGY CHANGES AND DYNAMICAL EFFECTS

The recognition of the critical lines bounding $\mathcal{L}$ together with some numeric simulations of the reduced phase space $\mathcal{P}$ (see the figure pairs 1 and 2), enable us to determine the influence of τ and ν on the topology of $\mathcal{P}$, namely on the structure of orbit bundles of the TC dynamics.

For $(\nu, \tau) \in \mathcal{L}$, the fixed points resulting from Eqs. (8), with $\sigma = +1$, consist of two maxima M_-, M_+ and a saddle M_0 such that $\theta = \pi/2$ and $X_- < X_0 < X_+$. Such a situation [17] is described in Fig. 1a and Fig. 1b where, with $\tau = 0.5$, the cases $\nu = 0.25$ and $\nu = 0.75$, respectively, are depicted. Their symmetric structure under the global reflection with respect to the axis $D/N = 0$, reflects the symmetry of Hamiltonian H_0 which combines the changes $\nu \to 1-\nu$ and $D \to -D$.

When $\tau = const$ and $\nu \to \nu_1^-$ $(\nu \to \nu_2^+)$, a *coalescence effect* takes place in which M_- (M_+) and M_0 merge in a unique point. This process can be driven either by the potential-depth gap $w = v_2 - v$ or by the total boson number N through the parameter $\nu = w/UN$ (notice that U, accounting for the s-wave scattering length, in the present paper is considered as a fixed parameter). The presence of the adjustable gap w, however, allows one to operate leaving N (and thus $\tau = T/UN$) unchanged. Fig. 2a and Fig. 1b illustrate the effect of crossing the $\mathcal{L}$ border by changing ν from 1 to 0.75. No change of the $\mathcal{P}$ structure occurs by further decreasing ν as far as $\nu_1(\tau) < \nu$. Fig. 1a and Fig. 1b, in fact, have the same number of extremal points.

Thanks to the presence of τ, the coalescence can be achieved as well if, keeping ν constant within the interval $-1 < \nu < 2$, the change $\tau \to \tau' > \tau$ is such that $(\nu, \tau) \in \mathcal{L}$ while $(\nu, \tau') \notin \mathcal{L}$. The comparison of Fig. 1a and Fig. 2b, both having $\nu = 0.25$, well illustrates the phase-space structure emerging from the coalescence of M_+ with the saddle M_0 as a consequence of the change $\tau = 0.5 \to \tau' = 1$.

The *orbit-bundle* structure deeply reflects the action of ν-τ changes. For $(\nu, \tau) \in \mathcal{L}$, $\mathcal{P}$ displays *five* independent bundles whose topology is characterized by means of three separatices (dashed lines in all the figures) $\mathcal{S}_+$, $\mathcal{S}_-$, and $\mathcal{S}_0$ (the latter shows a γ shape). Outside $\mathcal{L}$, owing to the coalescence (see Figs. 2a, 2b), separatrix $\mathcal{S}_0$ disappears, while the orbit bundles reduce to *three*. Curves $\mathcal{S}_\pm$ are easily identified by observing that they start/terminate at $D = \pm N$, $\theta = \pi/4$, $3\pi/4$, whereas $\mathcal{S}_0$ is based at $D = NX_0$, $\theta = \pi/2$, where X_0 is given by Eqs. (8). Notice that for $\nu < 0.5$ the two basins encircled by $\mathcal{S}_+$ and $\mathcal{S}_-$ contain the minimum m and the maximum M_-, respectively (see Figs. 1a, 2b), while the opposite situation appears for $\nu > 0.5$ (see Figs. 1b, 2a), where $\mathcal{S}_+$ and $\mathcal{S}_-$ encircles M_+ and m, respectively. In both cases, such basins are filled by closed-curve bundles entailing *bounded* oscillations for θ.

Two bundles of *ballistic* orbits, instead, are comprised between $\mathcal{S}_+$ and $\mathcal{S}_-$ and separated by $\mathcal{S}_0$ when $(\nu, \tau) \in \mathcal{L}$. In this case, no constraint limits θ that covers its whole range $[0, 2\pi]$, as shown by Figs. 3a, and 4a. The closed arc $\mathcal{C}_0$, constituting the noose of $\mathcal{S}_0$, confines a further closed-orbit bundle that encircles M_+ (M_-) for $\nu < 0.5$ $(\nu > 0.5)$.

When the coalescence is enacted, $\mathcal{C}_0$ and the basins around $M_\pm$ collapse, while $\mathcal{S}_0$ merges to the ballistic-curve flows lying between $\mathcal{S}_-$ and $\mathcal{S}_+$ (see Figs 2a, 2b). This topology change is accompanied by another, dynamically relevant, effect that consists of the suppression of the two motion curves forming $\mathcal{S}_0$: the closed branch $\mathcal{C}_0$ and the Λ-shaped branch. Such orbits, both starting and terminating at M_0, are characterized by an *infinite* covering time (illustrated in the following sub-section) as required by the saddle feature of M_0. Orbits placed in their proximity, which before the coalescence display arbitrarily long percurrence times, lose such a character after the saddle suppression. A special macroscopic trait therefore distinguishing the parameter choices $(\nu, \tau) \in \mathcal{L}$ and $(\nu, \tau) \notin \mathcal{L}$ is that the former choice always involves the presence of nonzero set of initial conditions around M_0 whose characteristic time period can become arbitrarily large. This feature, of course, is interesting both for achieving a complete control of the TWS characteristic times and in view of the experimental observations.

Ballistic motion and self-trapping. In Figs. 3, where the elapsing time is UNt, we illustrate the evolution of both D/N (its oscillations are evidenced in the grey stripe) and θ relevant to various orbits in $\mathcal{P}$. In Fig. 3a, D/N and θ are given for two orbits having energy values E_A, E_B, with $\tau = 0.5$, $\nu = 0.25$. These energies are such that $E_A - E_B \simeq 5 \cdot 10^{-4} E_0$, where E_0 is the energy of $\mathcal{S}_0$ and $|E_B - E_0| \simeq 10^{-9} E_0$. The period of the E_B orbit is greater than that of the E_A orbit since the former is closer to $\mathcal{S}_0$. Both θ and D/N exhibit an intermittent evolution where time changes are confined in a sub-interval of the characteristic period in which rapid *population inversion* effects are visible as well. Fig. 3b shows D/N and θ for two orbits near m, and M_- and allows one to compare the corresponding periods with the ballistic motions of Fig. 3a. The evolution of θ and D/N is displayed in Fig. 4a for an orbit almost coinciding with $\mathcal{S}_0$ (rapid local variations of both are visible in correspondence to the motion around the $\mathcal{S}_0$ noose). Fig. 4b shows θ and D/N for two orbits near $\mathcal{S}_-$ for $\tau = 1$, $\nu = 0.25$: the inner orbit exhibits a pulsed population inversion where abrupt changes alternate with an almost linear decreasing of D/N.

In consequence of the two-parameter dependence of the $\mathcal{P}$ topology, also the *self-trapping* effect can be induced/suppressed through τ and ν. We recall that the latter is particularly evident [5, 6] when the phase space displays pairs of isoenergetic orbits. In this case the system is imposed to single out one of the available orbits at a given energy. This symmetry breaking effect entails the self-trapping in a restricted region of $\mathcal{P}$ which cannot be left unless sufficiently large energy changes are effected.

In the presence of two, well separated maxima M_- and M_+ (Fig. 1a and Fig. 1b), the self-trapping regimes exhibit oscillations of populations $n_i = |z_i|^2$ such that either $n_1 = n_3 \simeq 0$, $n_2 \simeq N$ (orbits close to M_- with $D \simeq -N$) or $n_1 = n_3 \simeq N/2$, $n_2 \simeq 0$ (orbits close to M_+ with $D \simeq N$). As a result, the trajectories encircling the maximum manifest an evident, stable population imbalance (namely $n_1 = n_3 >> n_2$, $n_1 = n_3 << n_2$) during the system evolution that excludes the oscillations to approach intermediate states $n_1 = n_3 \simeq N/4$, $n_2 \simeq N/2$ $(D \simeq 0)$ near the minimum energy configuration m. We wish to notice that, when the suppression happens and M_- (M_+) and M_0 merge in a unique point, in general, the remaining maximum M_+ (M_-) keeps a position that is rather different from that of the minimum (see Fig. 2a, Fig. 2b) and thus preserves a regime with a marked population imbalance.

Concerning the change $\nu \to 1 - \nu$ $(\Leftrightarrow \; D \to -D)$ it is worth noting that, while the basins of M_0 and $M_\pm$ remain unaltered, the ballistic orbit bundles between $\mathcal{S}_+$ and $\mathcal{S}_-$ undergo an abrupt inversion. For $\nu = 0.5$ the linear D term in H_0 disappears and the resulting symmetry $D \to -D$ renders the dimeric regime of the open TWS equivalent to the pure symmetric dimer [4, 6]. We devote a final remark to the case $\nu = 0$ (equal well depths). Since $(\tau, \nu) \notin \mathcal{L}$ for any $\tau \neq 0$ if $\nu = 0$, then $\mathcal{P}$ portraits are quite similar to the one of Fig. 2b showing the ballistic phase evolution and pulsed population inversions (see Fig. 4b). It is worth noting that the evident asymmetric character of the TWS dynamics, well displayed by the $\mathcal{P}$ portraits, ensues not only from the well-depth diversity but also from the fact the pair of TC is described within the integrable regime by an unique collective variable z.

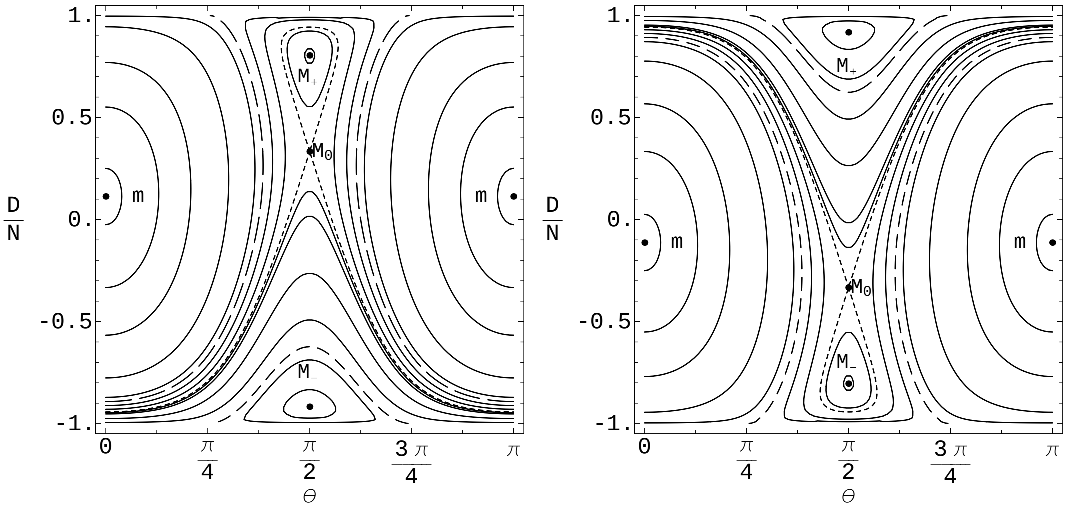

Figure 1: (a) Left figure is obtained by setting $\tau = 0.5$, $\nu = 0.25$; (b) right figure corresponds to $\tau = 0.5$, $\nu = 0.75$. In both figures, the minimum m, the saddle M_0 and the maxima $M_\pm$ are visible as well as separatrices $\mathcal{S}_0$, $\mathcal{S}_\pm$ represented by different dashing styles.

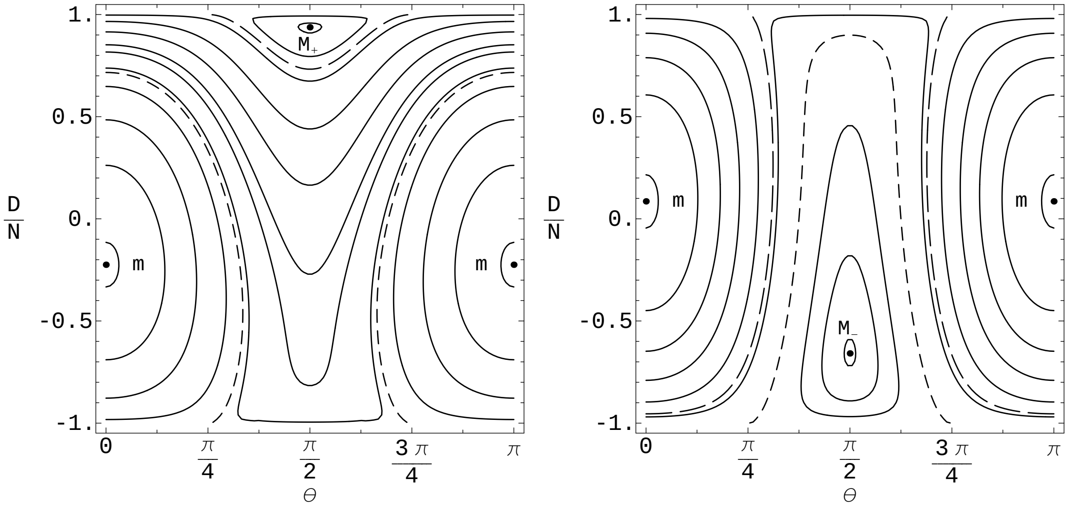

Figure 2: (a) Left figure illustrates $\mathcal{P}$ for $\tau = 0.5$, $\nu = 1$: increasing ν from $\nu = 0.75$ causes the coalescence of M_0 and M_- displayed in Fig. 1b. (b) Right figure corresponds to $\tau = 1$, $\nu = 0.25$: increasing τ from the value $\tau = 0.5$ causes the coalescence of M_0 and M_+ displayed in Fig. 1a.

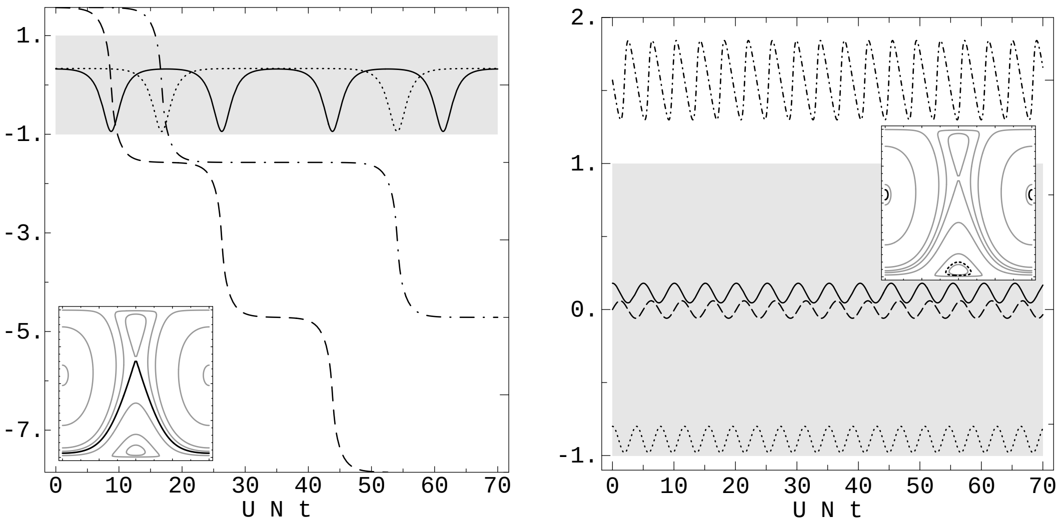

Figure 3: Evolutions of $D/N \in [-1, 1]$ (in the grey stripes) and θ for some orbits in $\mathcal{P}$ (see the sub-panels), with $\tau = 0.5$, $\nu = 0.25$; UNt is the rescaled time. (a) Left figure: θ and D/N for two orbits very close to the Λ branch of $\mathcal{S}_0$. The orbit closer to $\mathcal{S}_0$ has a larger period. (b) Right figure: periods of left-figure orbits can be compared with those of two orbits near M_- and m. Refer to the text for further comments.

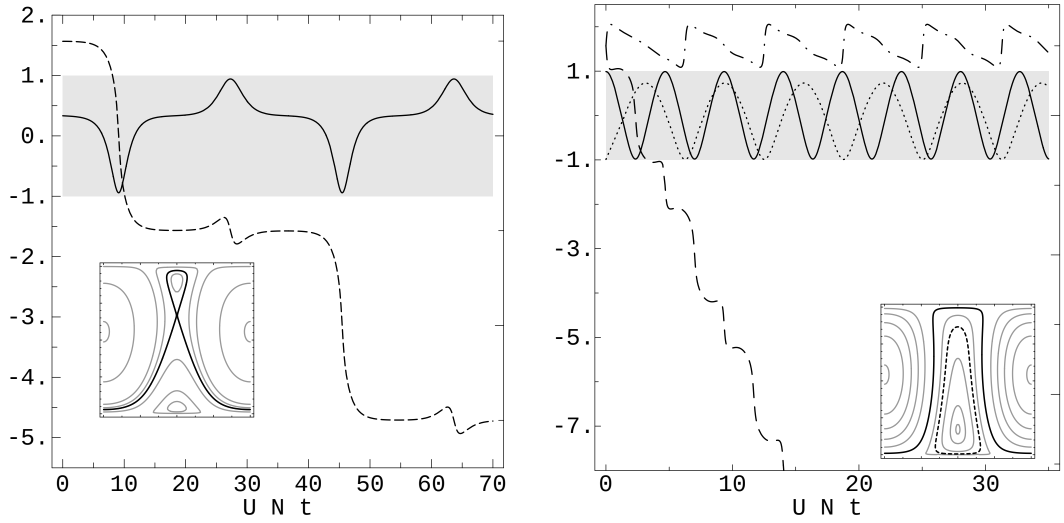

Figure 4: Evolutions of $D/N \in [-1, 1]$ (evidenced in the grey stripes) and θ for various orbits in $\mathcal{P}$ (see the sub-panels). UNt is the rescaled time (a) Left figure corresponds to an orbit very near $\mathcal{S}_0$, with $\tau = 0.5$, $\nu = 0.25$. (b) Right figure shows two orbits adjacent to $\mathcal{S}_-$ with $\tau = 1$, $\nu = 0.25$.

5. QUANTUM APPROACH TO DIMERLIKE DYNAMICS

The trimer dynamics naturally undergoes a quantum formulation both when it is investigated in the low-energy regime and if small particle numbers per well do not allow Bogolubov's approximation. Classically (namely in the mean-field picture described in section 2), the ground-state configuration is fully determined and represents a special case within the dimeric regime. In the alternative canonical scheme discussed above, quantum Hamiltonian (1) takes the form ($n_c := c^\dagger c$, $c = a, b$)

$$H = U \left[n_2^2 + \tfrac{1}{2}(n_a + n_b)^2 + \tfrac{1}{2}(b^\dagger a + a^\dagger b)^2 \right]$$

$$-v(n_a + n_b) - w n_2 - \frac{T}{\sqrt{2}} \left(a_2 a^\dagger + a_2^\dagger a \right) ,$$

where the quantum counterparts of new variables ξ, z are

$$b = (a_1 - a_3)/\sqrt{2}, \quad a = (a_1 + a_3)/\sqrt{2} ,$$

obeying the commutators $[b, b^\dagger] = 1 = [a, a^\dagger]$. In the spirit of Bogolubov's approximation (which is valid when a bosonic mode c is strongly occupied so that $c^\dagger \simeq c^*$ and $c^\dagger c \simeq |c|^2$ with $[c, c^\dagger] \simeq 0$), we observe that for states close to the dimeric regime both a and a_2 are macroscopic, while b, $b^\dagger$ can be seen as microscopic degrees of freedom describing the deviation from the pure dimeric states. In particular, the classical condition $\xi \simeq 0$ should correspond quantally to have the expectation value $\langle b \rangle \simeq 0$, whereas $|\xi|^2$ -classically, the population of the ξ mode- should correspond to the operator n_b. Only quantum states involving small quantum numbers for n_b are expected to be excited in the system dynamics.

In the light of this, Eqs. (4) can be employed to approach in the appropriate way the dynamics in which b, and $b^\dagger$ are quantum objects, whereas a and a_2 can be identified with z and z_2, respectively, owing to their macroscopic character. The first two equations are in fact decoupled from the third one if one considers only the first order terms in ξ, ξ^*. Under such assumption the third equation, where $|\xi|^2\xi$ is now negligible, is independent in that the time evolution of z-dependent parameters is determined by the first two equations. Also, its form implies that $|\dot{\xi}| << |\dot{z}|$, $|\dot{z}_2|$ thus making ξ a slowly varying variable. This scenario suggests that the quantum problem for the ξ mode can be described by the Hamiltonian

$$H_b = \tfrac{U}{2}(2|z|^2 n_b + n_b^2) + \tfrac{U}{2}(b^\dagger z + z^* b)^2 - v n_b ,$$

where n_b^2 is negligible with respect to $2|z|^2 n_b$. The spectrum of H_b is easily calculated by recognizing that its spectrum generating algebra [18] is su(1,1). The latter is generated by

$$K_3 = (2n_b + 1)/4, \; K_+ = (b^\dagger)^2/2, \; K_- = (K_+)^\dagger,$$

with commutators $[K_3, K_\pm] = \pm K_\pm$, $[K_-, K_+] = 2K_3$. Upon noticing that $(b^\dagger z + z^* b)^2 = z^2 (b^\dagger)^2 + (z^*)^2 b^2 + |z|^2(2n_b + 1)$, one gets H_b in the new form

$$H_b = 2(2U|z|^2 - v)K_3 - \tfrac{U}{2}|z|^2$$

$$+U[z^2 K_+ + (z^*)^2 K_-] + \frac{v}{2} .$$

By using the unitary transformation $U_3 = \exp[i\phi K_3]$, (notice that $U_3 K_\pm U_3^\dagger = e^{\pm i\phi} K_\pm$), where ϕ is given by $z = |z| e^{i\phi}$, one finds that $H_b = U_3 H_* U_3^\dagger$ with

$$H_* = 2(2U|z|^2 - v)K_3 + 2U|z|^2 K_1 - \tfrac{U}{2}|z|^2 + \frac{v}{2} ,$$

where $K_1 = (K_+ + K_-)/2$ is one of the two noncompact generators of the pseudo-angular momentum standardly defined by means of $K_\pm = K_1 \pm iK_2$. The further transformation $U_2 = \exp[-i\alpha K_2]$ such that

$$U_2 K_3 U_2^\dagger = \mathrm{ch}(\alpha) K_3 + \mathrm{sh}(\alpha) K_1 ,$$

allows H_* to be expressed as

$$H_* = U_2 \left(R\, K_3 + - \tfrac{U}{2}|z|^2 + \frac{v}{2} \right) U_2^\dagger$$

$$= R\,\mathrm{ch}(\alpha)K_3 + R\,\mathrm{sh}(\alpha)K_1 - \tfrac{U}{2}|z|^2 + \frac{v}{2}$$

provided th$\alpha = U|z|^2/(2U|z|^2 - v)$ and $R^2 = (3U|z|^2 - v)(U|z|^2 - v)$, and either $|z|^2 > v/U$ or $|z|^2 < v/3U$ is fulfilled. Whenever one of the latter conditions is violated ($v/3U \le |z|^2 \le v/U$) the transformation U_2 must be related to the noncompact element K_1 (instead of K_3) in order to reproduce H_*. The ensuing effect is dramatic: While K_3 has a discrete, positive spectrum bounded from below,

$$spect(K_3) = (2n+1)/4\,, \quad n = 0, 1, 2, ...,$$

K_1 has a continuous, unbounded spectrum. Since we have used unitary transformations such spectra are those characterizing H_b itself. Therefore, only in the case when the initial conditions on z ensure the presence of a discrete spectrum

$$E_n(|z|^2) = \sqrt{(3U|z|^2 - v)(U|z|^2 - v)}\,\frac{(2n+1)}{4}$$
$$-\tfrac{U}{2}|z|^2 + \frac{v}{2}$$

the ground-state turns out to be stable in that an energy gap separates it from the first excited state. This makes stable the dimeric regime. A final check is quite natural at this point. Making use of the first of eqs. (4) in the integrable subdynamics ($\xi = 0$) and recalling that $z = \sqrt{2}\,z_1$, the discreteness condition becomes

$$\left(4U\,|z_1|^2 + \frac{T}{2}\frac{z_2}{z_1}\right)\frac{T}{2}\frac{z_2}{z_1} \ge 0 \qquad (9)$$

Remarkably, the conditions on the Hamiltonian parameters τ and ν enforcing condition (9) are basically the same ensuring that the classical fixed points are stable. That is to say, the discreteness condition (9) selects the stable regions (maxima and minima) of the dimeric stability diagram appearing in ref. [13].

We briefly recall that, owing to a global phase symmetry, each dimeric fixed point can be identified by a pair of real numbers, x_1 and x_2, such that $z_1 = z_3 = \sqrt{N}\,x_1$ and $z_2 = \sqrt{N}\,x_2$. It proves then useful to introduce the real parameter $\alpha = x_2/(\sqrt{2}x_1)$ such that $x_1 = \cos(\vartheta)/\sqrt{2}$, $x_2 = \sin(\vartheta)$, where $\vartheta = \arctan\alpha$. This way each fixed point is uniquely related to a single real parameter, either ϑ or $\alpha = \tan\vartheta$. It turns out that, for a given choice $\tilde{\tau}$,$\tilde{\nu}$ of the parameters, the relevant ϑ's can be found by intersecting the straight line $\tau = \tilde{\tau}$ and the curve $\tau = \max[0, \tau_{\tilde{\nu}}(\vartheta)]$, where $\tau_\nu(\vartheta) = [\nu + 1 + \alpha^2(\nu - 2)]/(\alpha^4 - 1)$. If $\vartheta > 0$ the relevant fixed point is a minimum. Conversely, if $\vartheta \le 0$, it is either a maximum or an unstable [20] saddle depending on whether $\tilde{\tau} > \bar{\tau}(\vartheta)$ or $0 < \tilde{\tau} < \bar{\tau}(\vartheta)$, where $\bar{\tau}(\vartheta) = \max[\tau_1(\vartheta), \tau_2(\vartheta)]$,

$$\tau_1(\theta) = \frac{-2\sqrt{2}}{\beta\,(1+\beta^2)},\ \ \tau_2(\theta) = \frac{-6\sqrt{2}\beta^3}{(1+\beta^2)^3}, \qquad (10)$$

with $\beta = \tan\theta$. Now, recalling that $T = UN\tau$, equation (9) finally reduces to

$$[2\tau\tan\theta/(1+\tan^2\theta) + \tau^2\tan^2\theta/\sqrt{2}] \ge 0 \quad (11)$$

which selects the minima and, almost exactly, the maxima regions defined by the study of the stability character of the classical fixed points above recalled. Indeed the points in the minima region, $\{0 < \vartheta < \pi/2, \tau \ge 0\}$, trivially meet condition (11). The same is true for most of the maxima region, $\{-\pi/2 < \vartheta < 0, \tau > \bar{\tau}(\vartheta)\}$. Indeed, if $\vartheta < 0$, condition (11) selects the region above $\tau_1(\vartheta)$, which is exactly the borderline between maxima and saddles when $\tau_1(\theta) > \tau_2(\theta)$. In the complementary case, $\tau_1(\theta) < \tau_2(\theta)$, a small portion of the saddles region is predicted to give rise to a discrete rather than continuous spectrum. This slight disagreement can be tentatively explained by observing that in the latter case ϑ (is likely to be) can be quite close to $-\pi/2$, which ultimately means $|z_1| \sim 0$. This, however, is in contrast with our hypothesis that z_1 is macroscopic.

5. CONCLUSIONS

Based on a variational technique previously developed [6, 14], we have studied the integrable sub-regime of the TWS dynamics in terms of the expectation value z_i (z_i^*) relevant to operators a_i ($a_i^\dagger$). Our approach is equivalent to the standard mean-field picture. Upon defining suitable collective canonical modes, in section 2 we have presented an alternative description of the dynamics which allows to project the TWS dynamics on the reduced ($z_1 = z_3$) space $\mathcal{P}$ containing the integrable orbits, and avoids the nontrivial Dirac's method for constrained hamiltonian systems. The new picture thus obtained, in which TCs are always present, turns out to be equivalent to an asymmetric dimerlike model whose integrability is well known.

After deriving the fixed points of H_0 and the conditions determining the coalescence of fixed-point pairs depending on τ and ν (section 3), we have studied, in section 4, the TWS integrable sub-dynamics. The changes of the $\mathcal{P}$ topology and, more specifically, the changes of the structure of orbit bundles filling $\mathcal{P}$ have been considered under the variations of τ and ν, and the ensuing effects on dynamics have been dicussed. In particular, the ballistic orbit bundles have been found to have a periodic evolution whose time scale increases when the orbit approaches the separatrix $\mathcal{S}_0$. The possibility of having arbitrarily large time periods for a nonzero set of orbits disapperas as soon as a coalescence process destroys $\mathcal{S}_0$. Various situations in which the phase undergoes either a pulsed evolution or a stepwise variation while D/N shows rapid population inversions have been discussed. These effects share the common feature of being macroscopic, offer new information on the special TC regime of the three-well system, and thus are interesting in order to design new experiments on coupled BECs. The analysis we have performed on the $\mathcal{P}$ topology extends the study of the two-well dynamics [4], and recognizes the presence of the two-well phenomenology within the TWS dynamics. We notice that similar phenomena have been observed in the coherent-mode dynamics of weakly excited condensates [22], the motion equations of which exhibit in fact a rather similar nonlinear form.

We emphasize the fact that, beyond the rich scenario of dynamical behaviors, our analysis clearly displays both the way to prime macroscopic effects and the circumstances in which these are expected to occur by changing in a controlled way the relevant parameters N, τ and ν. In section 5 we have presented a preliminary study of the purely quantum TWS. A nice result which confirms the utility of the new canonical picture adopted in section 2 is that the algebraic analysis of the microscopic degrees of freedom capable of perturbing the integrable subregime permits to evidence the stable nature of TC configurations. These, in a sense, appear to be protected by the energy gap ensuing from the discrete form of the energy spectrum in the compact sector of the hamiltonian algebra su$(1,1)$. Noticeably, the noncompact sector giving a continuous spectrum turns out to characterize the system in correspondence to unstable TC states. A systematic quantum study of the TWS along the lines of Ref. [19], which is presently in progress, will be presented elsewhere.

ACKNOWLEDGEMENTS

The financial support of the INFM (Italy) and of the MURST is gratefully acknowledged.

References

[1] Ott, H. *et al.*, 2001 *Phys. Rev. Lett.* **87** 230401; Hänsel, W. *et al.*, 2001 *Nature* **413** 498; Reichel, J. 2002 *Appl. Phys.* B **75** 469.

[2] Pedri, P. *et al.*, 2001 *Phys. Rev. Lett.* **87** 220401; Morsch, O.*et al.*, 2001 *Phys. Rev. Lett.* **87** 140402.

[3] Milburn G.J. *et al.*, 1997 *Phys. Rev.* A **55** 4318; Steel, M.J. and Collet, M.J. 1998 *Phys. Rev.* A **57** 2920; Vardi, A. and Anglin, J.R. 2001 *Phys. Rev. Lett.* **86** 568.

[4] S. Raghavan *et al.*, 1999 *Phys. Rev.* A **59**, 620.

[5] Aubry, S.*et al.*, 1996 *Phys. Rev. Lett.* **76** 1607.

[6] Franzosi, R. *et al.*, 2000 *Int. J. Mod. Phys.* B **14** 943.

[7] Henning, D. *et al.*, 1997 *Phys. Rev.* E **51** 2870; Flach, S. and Fleurov, V. 1997 *J. Phys.: Condens. Matter* **9** 7039.

[8] Nemoto, K. *et al.*, 2001 *Phys. Rev.* A **63** 13604

[9] Franzosi, R. and Penna, V. 2002 *Phys. Rev.* A **65** 013601

[10] Jaksch, D. *et al.*, 1998 *Phys. Rev. Lett.* **81** 3108; Denschlag, J. *et al.*, 2000 *Science* **287** 97.

[11] Dalfovo, F. *et al.*, 1999 *Rev. Mod. Phys.* **71** 463, Legget, A.J. 2001 *Rev. Mod. Phys.* **73** 307.

[12] Franzosi, R. and Penna, V., 2003 *Phys. Rev.* E **67** 046227.

[13] Buonsante, P. *et al.*, *Phys. Rev. Lett.* **90** 050404.

[14] Amico, L. and Penna, V. 2000 *Phys. Rev.* B **62** 1224.

[15] Parkins, A.S. and Walls, D.F. 1998 *Phys. Rep.* **303** 1; Courteille, W. *et al.*, 2001 *Laser Physics* **11** 659.

[16] Penna, V. and Rasetti, M.G. 1994 *Phys. Rev.* B **50** 11783.

[17] We remark that points such as maxima $M_{\pm}$ in $\mathcal{P}$ might correspond to saddles in the full phase space $\mathcal{M}$. This information can be evinced from the analysis of Ref. [13]. Here, the standard terminology is used on $\mathcal{P}$ for the dimerlike dynamics, and serves to identify unambiguously extremal points of H_0.

[18] Penna, V. 1996 *Ann. of Phys.*, NY **245** 389.

[19] Franzosi, R. and Penna, V. 2001 *Phys. Rev.* A **63** 043609.

[20] The stability analysis evidences that the trimer may have stable saddle points. These, however, never have a dimeric character. See ref. [13] for further detail

[21] Zhang, W. M. *et al.*, 1990 *Rev. Mod. Phys.* **62** 867.

[22] Yukalov, V.I. *et al.*, 2002 *Phys. Rev.* A **66** 043602; Yukalov, V.I. *et al.* 2004 *Laser Phys.* **14** (to appear)